Arabian Journal of Geosciences (2018) 11: 586
https://doi.org/10.1007/s12517-018-3938-z

ORIGINAL PAPER

# Distribution rule of the in situ stress state and its influence on the permeability of a coal reservoir in the southern Qinshui Basin, China

Chenlin Wang [1] · Xiaodong Zhang [1,2]

Received: 9 July 2018 / Accepted: 24 September 2018 / Published online: 3 October 2018


**Abstract**
The recent development of the coalbed methane (CBM) industry has a significant role in advancing hydraulic fracturing theory and technology. However, further development requires a better understanding of how fractures influence reservoir permeability. In situ stress data from 54 CBM wells in the southern Qinshui Basin, China, were obtained by the injection/falloff test method to analyse the effect of in situ stress on the permeability of the CBM reservoir. The types of in situ stress states were classified, and the coal reservoir permeability under different in situ stress states was analysed. The results indicate that the maximum horizontal principal stress ($\sigma_H$), minimum horizontal principal stress ($\sigma_h$) and vertical principal stress ($\sigma_v$) all have positive linear relationships with the coal seam burial depth. Three in situ stress states were observed from the shallow to deep regions of the CBM reservoir in the study area: $\sigma_H > \sigma_h > \sigma_v$, $\sigma_H > \sigma_v > \sigma_h$ and $\sigma_v > \sigma_H > \sigma_h$, which account for 9, 76 and 15% of the test wells, respectively. Coal reservoir permeability decreases with increasing horizontal principal stress, whereas it first decreases with increasing $\sigma_v$, then increases and finally decreases. The variation in permeability with $\sigma_v$ is due to the conversion of the in situ stress states. Coal reservoir permeability has obvious differences under different in situ stress states. The permeability is the largest when $\sigma_v > \sigma_H > \sigma_h$, followed by $\sigma_H > \sigma_h > \sigma_v$ and smallest when $\sigma_H > \sigma_v > \sigma_h$. The permeability differences are caused by the fracture propagation shape of the rock strata under different in situ stress states.

**Keywords** In situ stress state · Coal reservoir · CBM · Permeability · Fracture propagation shape

## Introduction

The porosities and fractures of coal seams influence coalbed methane (CBM) accumulation zones and migration channels, therefore highlighting the importance of understanding these structural features to optimise CBM exploitation (Fan et al. 2010; Gerami et al. 2016; Mostaghimi et al. 2017). Previous studies have shown that the development of coal rock porosities and fractures is controlled by the coalification process and the geological evolution of the tectonic stress field, with the extension direction of the natural fractures primarily influenced by the modern tectonic stress state (Shen et al. 2014; Matsumoto et al. 2015; Guo et al. 2016).

In situ stresses consist of tectonic and gravitational stresses. The tectonic stresses, which extend horizontally, are classified into maximum and minimum horizontal stresses, whereas the gravitational stress extends vertically and originates from the overburden rock. The gravitational stress is therefore calculated as the product of the rock bulk density and depth (Brown and Hoek 1978; Hoek and Brown 1980). However, the tectonic stresses change with geological evolution of the strata and belong to the relatively complex spatial distribution of the unsteady stress field (Kang et al. 2009a, b). Determination of the stress field distribution is therefore important for estimating the geological structures and types of permeable fractures, both of which shape the production potential of CBM reservoirs (Gentzis 2009; Chatterjee and Pal 2010; Liu et al. 2016).

Permeability is the main reservoir parameter that determines CBM production. Numerous studies have observed the negative exponential relationship between the effective

✉ Chenlin Wang
wag_cheli@126.com

[1] School of Energy Science and Engineering, Henan Polytechnic University, Jiaozuo 454000, Henan Province, China

[2] Collaborative Innovation Center of Coalbed Methane (Shale Gas) in Central Plains Economic Zone, Jiaozuo 454000, Henan Province, China

stress and coal reservoir permeability (Connell et al. 2010; Yin et al. 2012; Shi et al. 2014a; Zhang et al. 2015; Zhao et al. 2015; Wang et al. 2017). A large number of permeability prediction models based on the effective stress have also been established (Pan and Connell. 2012; Xu et al. 2014; Chen et al. 2014; Shi et al. 2014b; Connell 2016). However, most of these models were developed under a pseudo/true triaxial stress state in laboratory settings. There are some significant differences between experimental and in situ coal seam conditions, such as the size of coal samples, the number and width of fractures and geological structures. Furthermore, the porosity and permeability of coal reservoirs are extremely low in China, which results in the permeability being highly sensitive to stress changes (Palmer and Mansoori 1996; Connell 2009; Lin and Kovscek 2014). This combination of the complicated in situ stress distribution, strong stress sensitivity to stress changes and low permeability complicates the feasibility of estimating CBM development potential. It is therefore necessary to study the spatiotemporal evolution of the in situ stress states throughout the targeted coal seam and its influence on coal reservoir permeability, which will provide a theoretical basis for CBM development in the study area.

In this paper, in situ stress data from 54 CBM wells in the southern Qinshui Basin, China, were obtained by the injection/falloff test method to study the distribution rule of the in situ stress state and its influence on coal reservoir permeability.

## Geological setting

The study area is located in the southern Qinshui Basin, Shanxi Province, China. The main tectonic features of the Qinshui Basin consist of a large NNE–SSW-striking complex syncline, some NNE-striking sub-folds and NE-striking sub-faults (Fig. 1). The northern extent of southern Qinshui Basin reaches 36° N, is fold- and fault-bounded around the rest of the basin and covers an area of approximately $1 \times 10^4$ km$^2$.

The main coal seams in the southern Qinshui Basin are the no.3 coal seam in the Permian Shanxi Formation and no.15 coal seam in the Upper Carboniferous Taiyuan Formation. The no.3 coal seam is distributed throughout the entire area, with an average coal seam thickness of 5.93 m that ranges from 2.4 to 8.1 m. It is the target zone of CBM development. The no.3 coal mainly consists of bituminous and anthracite coal with a high rank and $R_{o,max}$ values in the 1.87–4.26% range.

## Methodology

Injection/falloff well tests were used to acquire the coal reservoir parameters, such as the reservoir pressure, permeability and temperature. The injection/falloff well test procedure is as follows. Water is injected into the coal reservoir at a constant rate for 12 h and is then stopped, with the injection shut down for at least 24 h to obtain a complete injection/falloff curve. The bottom-hole pressure was measured using a down-hole pressure gauge during the injection and shut-in periods. The coal reservoir parameters were estimated by processing the injection/falloff curve. The straight-line analysis method and chart-board -matching analysis method were available to process the well test data. The straight-line analysis method was employed here. Pressure history matching curves were used to guarantee the validity of the data and confirm the results. However, the maximum injection pressure must be taken into account to obtain credible test results because of the impact stress has on the coal reservoir permeability. A minifrac test is therefore necessary to determinate the maximum injection pressure.

A multi-cycle hydraulic fracturing test was conducted to accurately calculate the breakdown and shut-in pressures. Two to three curves with better breakdown and shut-in effects were selected from the injection/falloff curves to calculate the parameter values. The pressure injection and pressure falloff curves were used to calculate the breakdown and shut-in pressures, respectively.

The breakdown and shut-in pressures of the coal reservoir were used to calculate the in situ stress parameters (Bredehoeft et al. 1976; Haimson and Cornet 2003). The horizontal principal stresses can be obtained from Eqs. (1) and (2):

$$p_c = \sigma_h \tag{1}$$

$$\sigma_H = 3p_c - p_f - p_0 + T \tag{2}$$

where $\sigma_h$ and $\sigma_H$ represent the minimum and maximum horizontal principal stresses (MPa), respectively; $p_c$ is the fracture shut-in pressure (MPa); $p_f$ is the breakdown pressure of the coal seam (MPa); $p_0$ is the reservoir pressure (MPa); and $T$ is the tensile strength of the coal seam (MPa).

The fracture was fractured repeatedly to obtain the reopened fracture pressure from the multi-cycle hydraulic fracturing process. The tensile strength of the coal seam approached zero after the coal seam fractured, and the reopened pressure of fracture could be expressed as:

$$p_r = 3p_c - \sigma_H - p_0 \tag{3}$$

where $p_r$ is the reopened fracture pressure (MPa).

The computational formula for the tensile strength was obtained by substituting Eqs. (1) and (3) into Eq. (2) as follows:

$$T = p_f - p_r \tag{4}$$

The vertical principal stress is mainly due to the weight of the overlying rock strata. The vertical principal stress can be

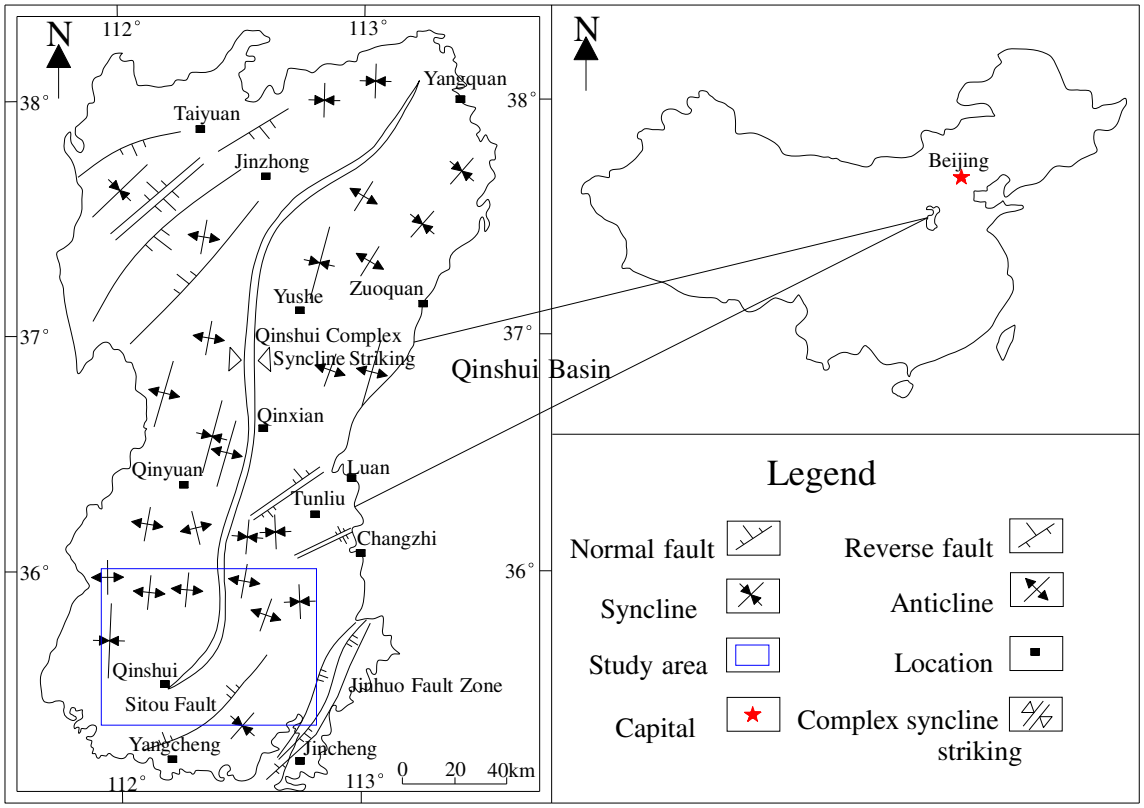


**Fig. 1** Geological structure map of the Qinshui Basin, China, and the location of the study area

calculated from Eq. (5) (Brown and Hoek 1978; Hoek and Brown 1980):

$$\sigma_v = \gamma H = 0.027H \tag{5}$$

where $\sigma_v$ is the vertical principal stress (MPa); $\gamma$ is the rock bulk density (kN/m$^3$); and $H$ is coal seam depth (m).

The positive linear relationships between the coal seam depth and the reservoir, breakdown and the shut-in pressures are shown in Fig. 2. The fitting formulas are as follows:

$$p_0 = 0.01H - 2.2726 \tag{6}$$

$$p_f = 0.0182H + 3.2136 \tag{7}$$

$$p_c = 0.0178H + 2.6093 \tag{8}$$

## Results

### Test parameters

The relevant parameters for the test data from the 54 CBM wells that sampled the no.3 coal seam in the southern Qinshui Basin are listed in Table 1.

The test results (Table 1) indicate that the initial reservoir pressure gradient ($\delta_0$) is 0.07–1.08 MPa/100 m, with a mean value of 0.70 MPa/100 m, and 96% of the test wells possessing a pressure gradient that is lower than the hydrostatic gradient (0.98 MPa/100 m). The coal reservoir permeability is 0.01–1.02 mD, with a mean value of 0.14 mD, and 98% of the test wells yielding values lower than 1 mD. The coal reservoir in the study area should therefore be classified as an underpressured, low-permeability reservoir according to Pashin (2007) and Mazumder et al. (2012).

### The distribution rule of the in situ stress state

Positive linear relationships exist between the coal seam depth and the maximum and minimum horizontal principal stresses, as shown in Fig. 3. The relevant relationships are as follows:

$$\sigma_H = 19.303H + 281.71 \tag{9}$$

$$\sigma_h = 35.348H + 211.17 \tag{10}$$

Three different in situ stress states are observed in the study area, as shown in Fig. 4. For $\sigma_H > \sigma_h > \sigma_v$, the coal seam depth ranges from 518 to 846 m, with a mean depth of 626 m. For $\sigma_H > \sigma_v > \sigma_h$, the coal seam depth ranges from 461 to 1272 m, with a mean depth of 828 m. For $\sigma_v > \sigma_H > \sigma_h$, the coal seam depth ranges from 641 to 1423 m, with a mean value of 905 m. The in situ stress states of the coal seam from its shallow to

**Table 1** Injection/falloff and in situ stress test parameters in the study area (the range and mean of each parameter value are provided)

| | Parameters | Values |
|---|---|---|
| Injection/falloff well test parameters | Burial depth (m) | 461.19–1422.75 (822.01) |
| | Reservoir pressure (MPa) | 0.39–11.32 (5.92) |
| | Reservoir pressure gradient (MPa/100 m) | 0.07–1.08 (0.70) |
| | Temperature (°C) | 12.07–38.84 (27.61) |
| | Temperature gradient (°C/100 m) | 2.21–5.35 (3.45) |
| | Permeability (mD) | 0.01–1.02 (0.14) |
| Multi-cycle hydraulic fracturing test parameters | Shut-in pressure (MPa) | 9.69–29.04 (17.24) |
| | Shut-in pressure gradient (MPa/100 m) | 1.24–3.08 (2.13) |
| | Breakdown pressure (MPa) | 10.49–31.38 (18.18) |
| | Breakdown pressure gradient (MPa/100 m) | 1.49–3.19 (2.25) |
| In situ stress parameters | Maximum horizontal principal stress (MPa) | 13.29–44.87 (27.76) |
| | Maximum horizontal principal stress gradient (MPa/100 m) | 1.69–5.44 (3.46) |
| | Minimum horizontal principal stress (MPa) | 9.69–29.09 (17.15) |
| | Minimum horizontal principal stress gradient (MPa/100 m) | 1.24–3.08 (2.12) |
| | Vertical principal stress (MPa) | 12.45–38.41 (22.07) |
| | Tensile strength (MPa) | 0.09–0.93 (0.55) |

deep extent are therefore $\sigma_H > \sigma_h > \sigma_v$, $\sigma_H > \sigma_v > \sigma_h$ and $\sigma_v > \sigma_H > \sigma_h$, respectively.

The quantity and percentage of the different in situ states in the study area are shown in Fig. 5. There are five CBM wells where $\sigma_H > \sigma_h > \sigma_v$, which accounts for 9% of the test wells. There are 41 CBM wells where $\sigma_H > \sigma_v > \sigma_h$, which accounts for 76% of the test wells. There are eight CBM wells where $\sigma_v > \sigma_H > \sigma_h$, which accounts for 15% of the test wells. The in situ stress state of the coal seam is therefore dominated by $\sigma_H > \sigma_v > \sigma_h$ in the study area.

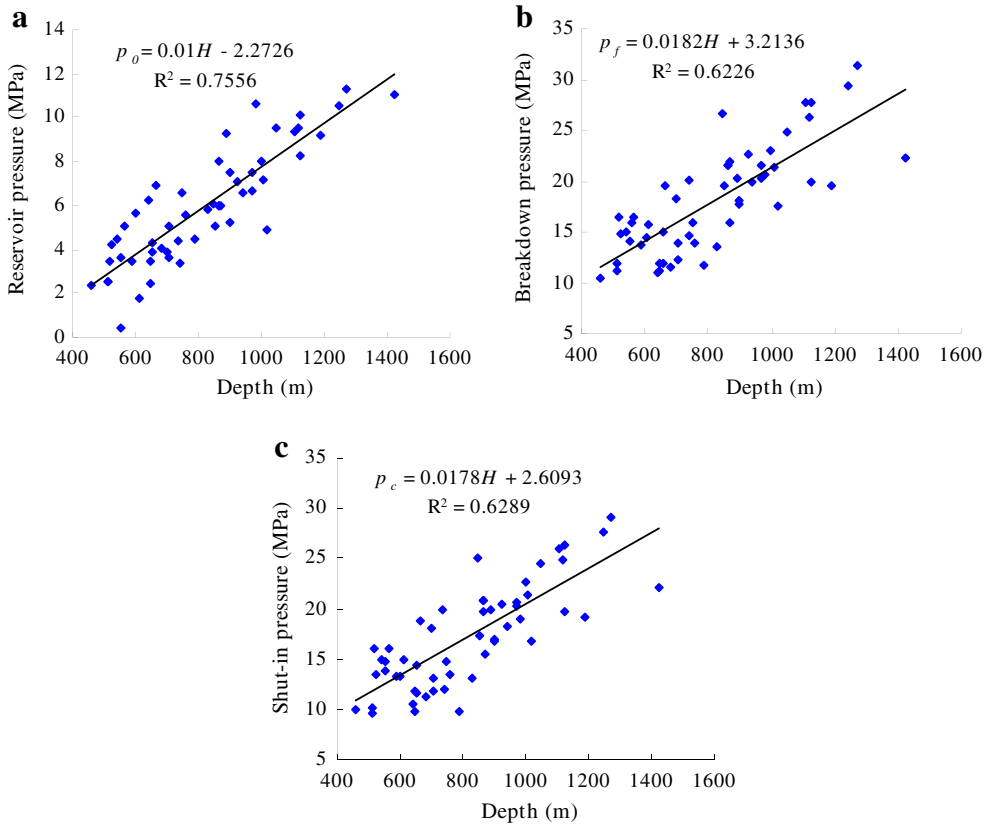


**Fig. 2** Relationship between the injection/falloff test parameters and coal seam depth. a Relationship between the reservoir pressure and coal seam depth. b Relationship between the breakdown pressure and coal seam depth. c Relationship between the shut-in pressure and coal seam depth

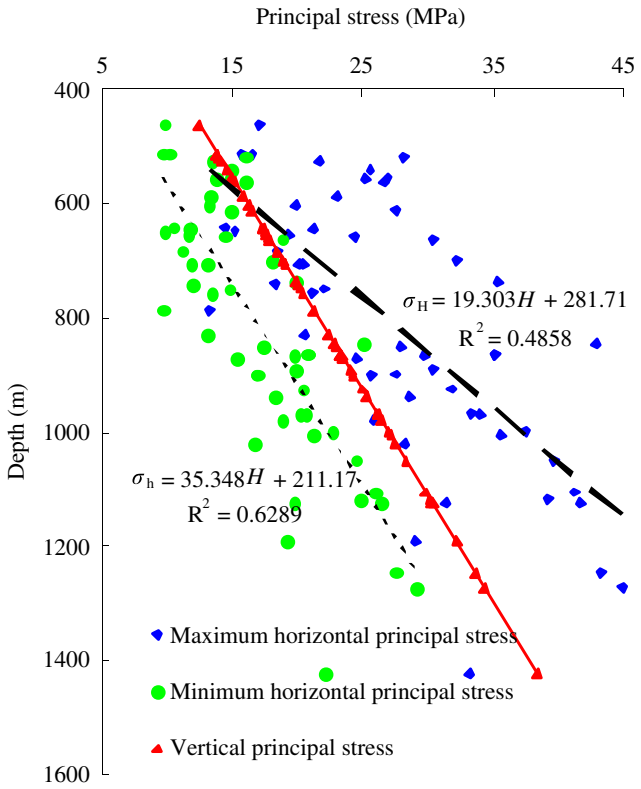


**Fig. 3** Relationships between the principal stresses and coal seam depth

## The influence of the in situ stress state on permeability

Coal reservoir permeability directly influences the productivity of a CBM well. Field and laboratory tests both show that there is a negative exponential relationship between the coal reservoir permeability and effective stress as follows (Connell et al. 2010; Yin et al. 2012; Shi et al. 2014a; Zhang et al. 2015; Zhao et al. 2015; Wang et al. 2017):

$$k = k_0 e^{-a\sigma_e} \tag{11}$$

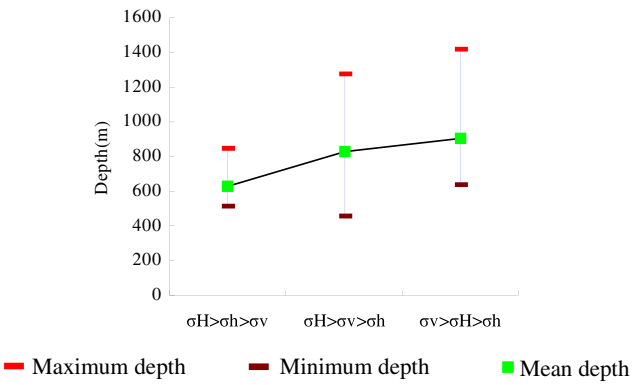


**Fig. 4** The coal seam depth under the different in situ stress states

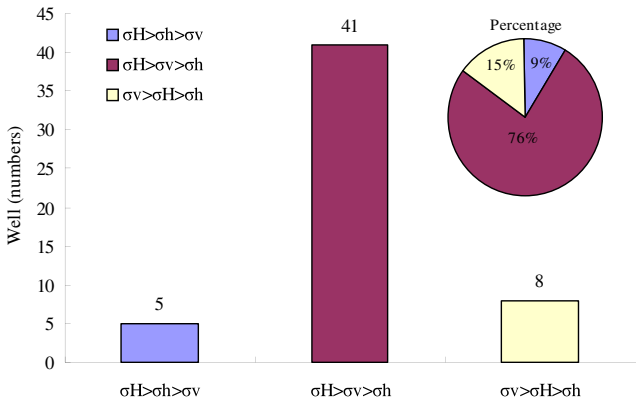


**Fig. 5** The quantity and percentage of the different in situ stress states

where $k$ represents the permeability (mD); $k_0$ is the initial permeability (mD); $\sigma_e$ represents the effective stress (MPa); and $\alpha$ is the fitting coefficient.

The variations in permeability with the principal stresses are analysed in Fig. 6. There is a rapid decrease in permeability with increasing $\sigma_H$ when $\sigma_H$ is less than 22 MPa, as shown in Fig.6a. The decrease in permeability slows down when $\sigma_H$ is greater than 22 MPa. The permeability rapidly decreases with increasing $\sigma_h$ when $\sigma_h$ is less than 15 MPa, as shown in Fig. 6b. The decrease in permeability slows down when $\sigma_h$ is greater than 15 MPa. The permeability first decreases with increasing $\sigma_v$, then increases and finally decreases, as shown in Fig. 6c. This indicates that the coal reservoir permeability variations due to $\sigma_v$ are relatively complex. The observed variation in permeability with $\sigma_v$ is consistent with that of Zhao et al. (2016).

The mean permeability exhibits a decrease-increase variation with the in situ stress states from the shallow to deep extent of the coal seam, as shown in Fig. 7. The mean permeability is lowest when $\sigma_H > \sigma_v > \sigma_h$, and the mean permeability is largest when $\sigma_v > \sigma_H > \sigma_h$. The mean permeability is intermediate when $\sigma_H > \sigma_h > \sigma_v$.

A comparison of Fig. 6c with Fig. 7 illustrates how the variation in permeability with $\sigma_v$ (< 24 MPa) has the same variation trend as the variation in mean permeability with the shallow to deep in situ stress states. The principal stresses continue to increase after $\sigma_v > \sigma_H > \sigma_h$, and the in situ stress state eventually reaches a hydrostatic stress state, where $\sigma_v = \sigma_H = \sigma_h$ (Hoek and Brown 1980). This results in the coal reservoir being under compression, which promotes fracture closure (Meng et al. 2010). This indicates that the coal reservoir permeability is extremely low when $\sigma_v = \sigma_H = \sigma_h$ and rapidly decreases after $\sigma_v > \sigma_H > \sigma_h$. The variation in permeability with the in situ stress states from the shallow to deep extent of the coal seam therefore follows a decrease-increase-decrease trend that is consistent with the variation in permeability with $\sigma_v$. The variation in permeability with $\sigma_v$ is due to the conversion of the in situ stress states.

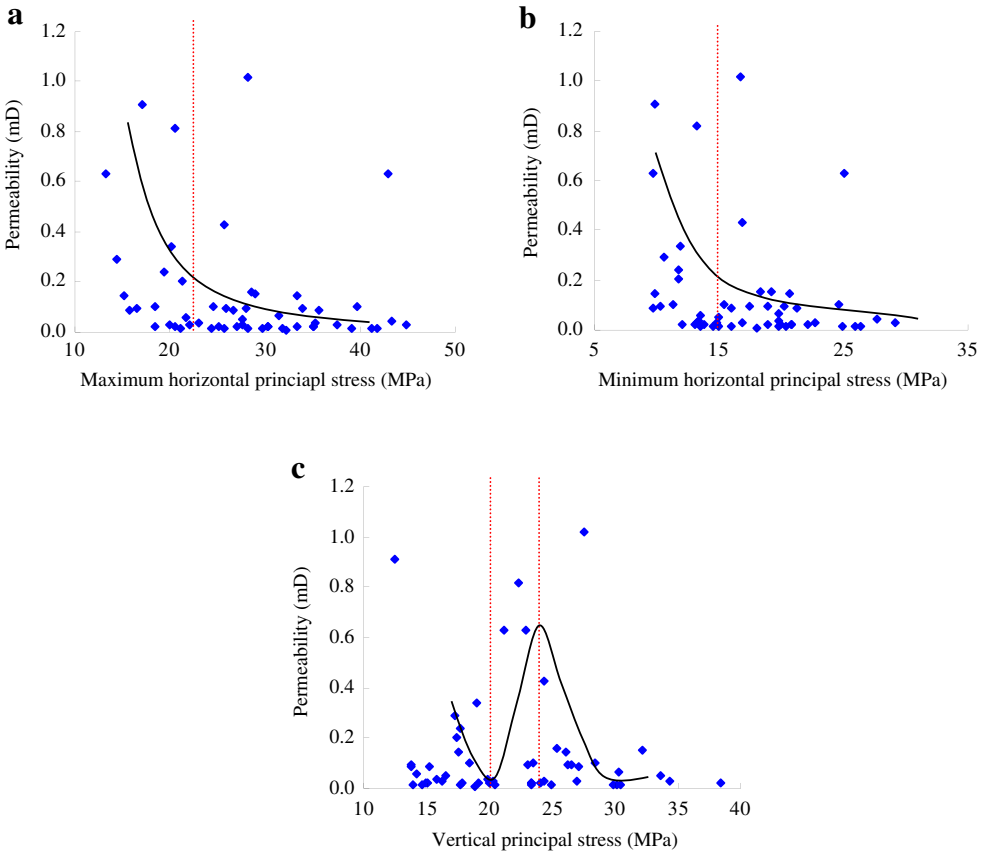


**Fig. 6** The variations in permeability with the principal stresses. **a** The variation in permeability with the maximum horizontal principal stress. **b** The variation in permeability with the minimum horizontal principal stress. **c** The variation in permeability with the vertical principal stress

## Discussion

Anderson's three stress regimes classified the in situ stress states into normal stress, strike-slip and thrust regimes (Anderson 1951). $\sigma_v$ is the largest principal stress in the normal stress regime, where $\sigma_v > \sigma_H > \sigma_h$. $\sigma_v$ is the intermediate principal stress in the strike-slip regime, where $\sigma_H > \sigma_v > \sigma_h$. $\sigma_v$ is the least principal stress in the thrust regime, where $\sigma_H > \sigma_h > \sigma_v$.

The strike-slip regime ($\sigma_H > \sigma_v > \sigma_h$) is conducive to forming a strike-slip fault, where the fracture propagation shape of the rock strata is shear fracture with horizontal movement, as shown in Fig. 8a. The normal stress regime ($\sigma_v > \sigma_H > \sigma_h$) is conducive to forming a normal fault, where the fracture propagation shape of the rock strata is tensile fracture with vertical movement, as shown in Fig. 8b. The thrust regime ($\sigma_H > \sigma_h > \sigma_v$) is conducive to forming a reverse fault, where the fracture propagation shape of the rock strata is shear fracture with vertical movement, as shown in Fig. 8c.

The mean permeability has obvious differences under the different in situ stress states, as shown in Fig. 7. The mean permeability decreases from $\sigma_H > \sigma_h > \sigma_v$ to $\sigma_H > \sigma_v > \sigma_h$, and the fracture propagation shape changes from shear fracture with vertical movement to shear fracture with horizontal

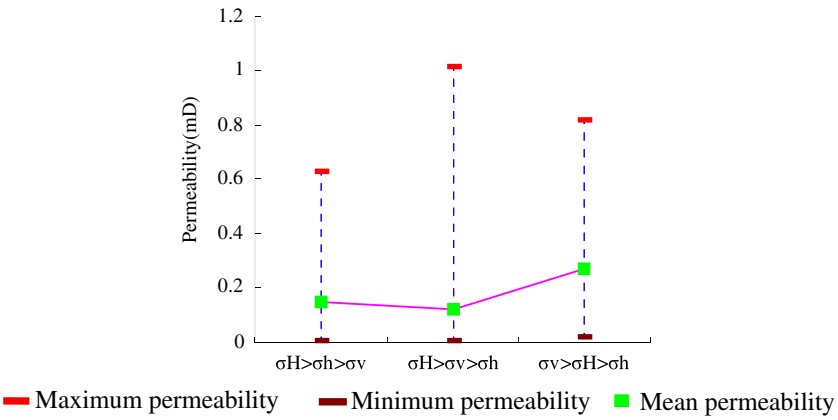


**Fig. 7** The variations in mean permeability under the different in situ stress states

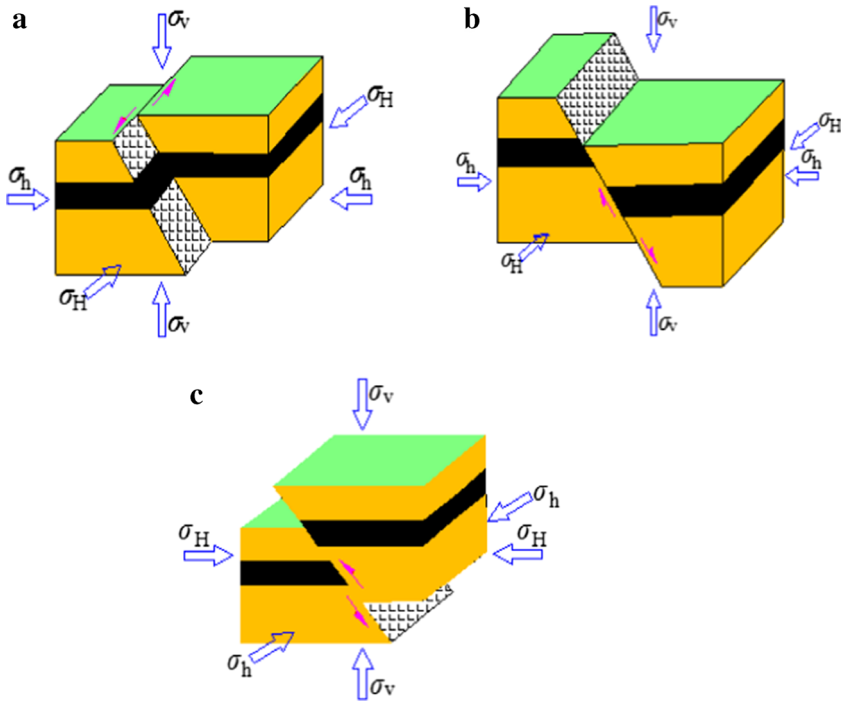


**Fig. 8** Tectonic settings under the different in situ stresses. **a** The strike-slip regime. **b** The normal stress regime. **c** The thrust regime

movement. This demonstrates that the horizontal movement of the coal seam decreases the coal reservoir permeability, whereas the vertical movement of the coal seam is conducive to enhancing the coal reservoir permeability. The mean permeability increases from $\sigma_H > \sigma_v > \sigma_h$ to $\sigma_v > \sigma_H > \sigma_h$, and the fracture propagation shape changes from shear fracture with horizontal movement to tensile fracture with vertical movement. This indicates that tensile fracture is conducive to enhancing the coal reservoir permeability. The permeability differences are therefore caused by the fracture propagation shape of rock strata.

## Conclusions

1. The maximum and minimum horizontal principal stresses have positive linear relationships with coal seam depth in the southern Qinshui Basin. The three in situ stress states are $\sigma_H > \sigma_h > \sigma_v$, $\sigma_H > \sigma_v > \sigma_h$ and $\sigma_v > \sigma_H > \sigma_h$ from the shallow to deep extent of the coal seam, respectively. The in situ stress state of the coal seam is dominated by $\sigma_H > \sigma_v > \sigma_h$ in the study area.
2. Coal reservoir permeability decreases with increasing horizontal principal stresses, whereas it first decreases with increasing $\sigma_v$, then increases and finally decreases. This variation in permeability with $\sigma_v$ is due to the conversion of the in situ stress states.
3. The permeability is the largest when $\sigma_v > \sigma_H > \sigma_h$, followed by $\sigma_H > \sigma_h > \sigma_v$ and smallest when $\sigma_H > \sigma_v > \sigma_h$ for the three different in situ stress states. The permeability differences are caused by the fracture propagation shape of the rock strata under different in situ stress states.

## References

Anderson EM (1951) The dynamics of faulting and dyke formation with application to Britain. Oliver and Boyd, London

Bredehoeft JD, Wolf RG, Keys WS et al (1976) Hydraulic fracturing to determine the regional in situ stress field in the Piceance Basin, Colorado. Geol Soc Am Bull 87:250–258

Brown ET, Hoek E (1978) Trends in relationships between measured in situ stresses and depth. Int J Rock Mech Min Sci Geomech Abstr 15(4):211–215

Chatterjee R, Pal PK (2010) Estimation of stress magnitude and physical properties for coal seam of Rangamati area, Raniganj coalfield, India. Int J Coal Geol 81(1):25–36

Chen Z, Liu JS, Pan ZJ et al (2014) Influence of the effective stress coefficient and sorption-induced strain on the evolution of coal permeability: model development and analysis. Int J Greenh Gas Control 8:101–110

Connell LD (2009) Coupled flow and geomechanical processed during gas production from coal seams. Int J Coal Geol 79(1–2):18–28

Connell LD, Lu M, Pan ZJ (2010) An analytical coal permeability model for tri-axial strain and stress conditions. Int J Coal Geol 84(2):103–114

Connell LD (2016) A new interpretation of the response of coal permeability to changes in pore pressure, stress and matrix shrinkage. Int J Coal Geol 162:169–182

Fan JJ, Ju YW, Hou QY et al (2010) Pore structure characteristics of different metamorphic deformed coal reservoirs and its restriction on recovery of coalbed methane. Earth Sci Front 17(5):325–335 (in Chinese)

Gentzis T (2009) Stability analysis of horizontal coalbed methane well in the Rocky Mountain Front Ranges of southeast British Columbia, Canada. Int J Coal Geol 77(3):328–337

Gerami A, Mostaghimi P, Armstrong RT, Zamani A, Warkaini ME (2016) A microfluidic framework for studying relative permeability in coal. Int J Coal Geol 159: 183–193

Guo P, Yao LH, Ren DS (2016) Simulation of three-dimensional tectonic stress fields and quantitative prediction of tectonic fracture within the Damintun Depression, Liaohe Basin, northeast China. J Struct Geol 86:211–223

Haimson BC, Cornet FH (2003) ISRM suggested methods for rock stress estimation-part 3: hydraulic fracturing (HF) and/or hydraulic testing of pre-existing fractures (HTPF). Int J Rock Mech Min Sci 40(7–8): 1011–1020

Hoek E, Brown ET (1980) Underground excavations in rock. The Institute of Mining and Metallurgy, London

Kang HP, Lin J, Yan LX et al (2009a) Study on characteristics of underground in-situ distribution in Shanxi coal mining fields. Chin J Geophys 52(7):1782–1792 (in Chinese)

Kang HP, Jiang TM, Zhang X et al (2009b) Research on in-situ stress field in Jincheng mining area and its application. Chin J Rock Mech Eng 28(1):1–8 (in Chinese)

Liu HH, Sang SX, Xue JH, Wang G, Xu H, Ren B, Liu C, Liu S (2016) Characteristics of an in situ stress field and its control on coal fractures and coal permeability in the Gucheng block, southern Qinshui Basin. China J Nat Gas Sci Eng 36(B):1130–1139

Lin WJ, Kovscek AR (2014) Gas sorption and the consequent volumetric and permeability change of coal I: experimental. Transp Porous Media 105(2):371–389

Matsumoto S, Nakao S, Ohkura T, Miyazaki M, Shimizu H, Abe Y, Inoue H, Nakamoto M, Yoshikawa S, Yamashita Y (2015) Spatial heterogeneities in tectonic stress in Kyushu, Japan and their relation to a major shear zone. Earth Planets Space 67:172

Mazumder S, Scott M, Jiang J (2012) Permeability increase in Bowen Basin coal as a result of matrix shrinkage during primary depletion. Int J Coal Geol 96-97(6):109–119

Meng ZP, Tian YD, Li GF (2010) Characteristics of in-situ stress field in Southern Qinshui Basin and its research significance. J Chin Coal Soc 35(6):975–981 (in Chinese)

Mostaghimi P, Armstrong RT, Gerami A, Hu Y, Jing Y, Kamali F, Liu M, Liu Z, Lu X, Ramandi HL, Zamani A, Zhang Y (2017) Cleat-scale characterization of coal: an overview. J Nat Gas Sci Eng 39:143–160

Palmer I, Mansoori J (1996) How permeability depends on stress and pore pressure in coalbeds: a new model. SPE Reserv Eval Eng 1(6):539–544

Pan ZJ, Connell LD (2012) Modelling permeability for coal reservoirs: a review of analytical models and testing data. Int J Coal Geol 92:1–44

Pashin JC (2007) Hydrodynamics of coalbed methane reservoirs in the Black Warrior Basin: key to understanding reservoir performance and environmental issues. Appl Geochem 22(10):2257–2272

Shen J, Qin Y, Fu XH et al (2014) Properties of deep coalbed methane reservoir-forming conditions and critical depth discussion. Nat Gas Geosci 25(9):1470–1476 (in Chinese)

Shi JQ, Durucan S, Shimada S (2014a) How gas adsorption and swelling affects permeability of coal: a new modeling approach for analyzing laboratory test data. Int J Coal Geol 128-129:134–142

Shi JQ, Pan ZJ, Durucan S (2014b) Analytical models for coal permeability changes during coalbed methane recovery: model comparison and performance evaluation. Int J Coal Geol 136:17–24

Wang BY, Qin Y, Shen J et al (2017) Study on stress sensitivity of lignite reservoir under salinity and pH composite system. Energy Explor Exploit 36(3):464–487

Xu H, Tang DZ, Tang SH, Zhao JL, Meng YJ, Tao S (2014) A dynamic prediction model for gas-water effective permeability based on coalbed methane production data. Int J Coal Geol 121:44–52

Yin GZ, Jinag CB, Xu J et al (2012) An experimental study on the effects of water content on coalbed gas permeability in ground stress fields. Transp Porous Media 94(1):87–99

Zhang ZT, Zhang R, Xie HP, Gao M (2015) The relationship among stress, effective porosity and permeability of coal considering the distribution of natural fractures: theoretical and experimental analyses. Enviro Earth Sci 73(10):5997–6007

Zhao JL, Tang DZ, Lin WJ, Xu H, Li Y, Tao S, Lv Y (2015) Permeability dynamic variation under the action of stress in the medium and high rank coal reservoir. J Nat Gas Sci Eng 26:1030–1041

Zhao JL, Tang DZ, Xu H, Li Y, Li S, Tao S, Lin W, Liu Z (2016) Characteristic of in situ stress and its control on the coalbed methane reservoir permeability in the eastern margin of the Ordos Basin, China. Rock Mech Rock Eng 49(8):3307–3322